FEATURE-BASED ANNEALING PARTICLE FILTER FOR ROBUST BODY POSE ESTIMATION

Adolfo López, Josep R. Casas
Image Processing Group, Technical University of Catalonia University, Barcelona, Spain
alopez@gps.tsc.upc.edu, jose[illegible]s.tsc.upc.edu

Keywords: Pose estimation, motion capture, particle filter

Abstract: This paper presents a new annealing method for particle filtering in the context of body pose estimation. The feature-based annealing is inferred from the weighting functions obtained with common image features used for the likelihood approximation. We introduce a complementary weighting function based on the foreground extraction and we balance the different measures through the annealing layers in order to improve the posterior estimate. This technique is applied to estimate the upper body pose of a subject in a realistic multi-view environment. Comparative results between the proposed method and the common annealing strategy are presented to assess the robustness of the algorithm.

1 INTRODUCTION

Markerless human motion capture is a challenging problem that involves estimating the high-dimensional configuration of a three-dimensional non-rigid and self-occluding object. Since a wide range of applications can be derived from the unobtrusive characterization of human activity, this research area is highly active.

A common model is an articulated body structure with several degrees of freedom that determine the dimensionality of the problem. With these kind of models one can simply adopt hard kinematic constraints or can go further restricting the motion, hence confining the solution to a more tractable subspace at the cost of generality loss. Regardless of the space in which we work, human dynamics present multi-modal non-linear and non-Gaussian statistics. Particle Filters (Arulampalam et al., 2002) have become a relevant technique due to their ability to precisely estimate the statistics of such processes. Several approaches such as partitioned sampling (MacCormick and Isard, 2000), hierarchical sampling (Mitchelson and Hilton, 2003) and annealing particle filter (Deutscher et al., 2000) have been developed to cope with high-dimensional limitations of the classical Condensation algorithm (Isard and Blake, 1998).

This paper presents a new annealing particle filter approach based on the properties of image features. The feature-based annealing concept exploits the attributes of the weighting functions generated by several measures constructed with common image features. We empirically show the increased robustness of our approach testing it under challenging conditions for human motion capture such as limited number of views and low frame rate.

2 PARTICLE FILTER

Particle Filters (PF) (Arulampalam et al., 2002) are recursive Bayesian estimators derived from Monte Carlo sampling techniques which can handle non-linear and non-Gaussian processes. Commonly used in tracking problems, they aim at estimating the posterior density $p(\mathbf{x}_t|\mathbf{z}_t)$ by means of a set of N_s weighted samples or particles:

$$p(\mathbf{x}_t|\mathbf{z}_t) \approx \sum_{i}^{N_s} w_t^i \delta(\mathbf{x}_t - \mathbf{x}_t^i) \quad (1)$$

where w_t^i is the weight associated to the i-th particle. This discrete approximation of the posterior requires the evaluation of weights. This is done by means of the importance sampling principle (Doucet et al., 2000), with a probability density function (pdf) $q(\mathbf{x}_t|\mathbf{z}_t)$ from which we generate samples that can be evaluated with the posterior (up to proportionality). This pdf is called the importance distribution.

After a certain time, the variance of the weights increases, causing what is known as particle degeneracy. This phenomena causes a degradation in the estimation. An effective measure for the particle degeneracy is the survival rate (Liu and Chen, 1998) given by:

$$\alpha = \frac{1}{N_s \sum_{i=1}^{N_s} (w_t^i)^2} \tag{2}$$

In order to avoid the estimator degradation, the particle set is resampled. After likelihood evaluation a new particle set must be drawn from the posterior estimation, hence particles with higher weights are reproduced with higher probability. Once the new set has been drawn, all the weights are set to $\frac{1}{N_s}$, leading to a uniformly weighted sample set concentrated around the higher probability zones of the estimated posterior.

2.1 Sampling Importance Resampling

The Sampling Importance Resampling (SIR) Particle Filter proposed in (Gordon et al., 1993) is a method commonly used in computer vision problems. It is characterized by applying resampling at every iteration and by defining the importance distribution as the prior density $p(\mathbf{x}_t^i|\mathbf{x}_{t-1}^i)$. By introducing these two elements, the computation of weights only depends on the likelihood.

$$w_t^i \propto p(\mathbf{z}_t|\mathbf{x}_t^i) \tag{3}$$

Consequently, the design of the particle filter is basically a problem of finding an appropiate likelihood function.

2.2 Annealing Particle Filter

It has been shown in several works that SIR Particle Filters are a good approach for tracking in low dimensional spaces, but they become inefficient in high-dimensional problems. Deutscher et. al (Deutscher et al., 2000) proposed a variation of the SIR framework by introducing the concept of Annealing PF. In body pose tracking problems, the likelihood approximation is often a function with several peaked local maxima. Annealing PF deals with this problem by evaluating the particles in several smoothed versions of the likelihood approximation. After the weights are computed via the modified likelihood, particles are resampled and propagated with Gaussian noise with zero mean and a covariance that decreases at every step. Each one of these steps (weighting with a smoothed function, resampling and propagation) is called an annealing run. In the last annealing run the estimation is given by means of the Monte-Carlo approximation of the posterior mean:

$$\hat{\mathbf{x}}_\mathbf{t} = \sum_{i=1}^{N_s} w_t^i \mathbf{x}_t^i \tag{4}$$

The most usual way to smooth the weighting function is by means of an exponent $\beta < 1$ called the annealing rate. In the first layer β is minimum, progressively increasing with each layer, sharpening the likelihood approximation. In (Deutscher et al., 2000) a method for tuning β with the survival rate after each annealing run is proposed.

The use of a hierarchical model (Canton-Ferrer et al., 2008) is another possible strategy in order to have annealing layers due to the exploration in spaces of increasing dimensionality.

Regarding the likelihood approximation, in (Deutscher et al., 2000) a matching of the model projection with foreground segmentation and edges is proposed. Their flesh model consists of conic sections with elliptical cross-sections surronding virtual skeleton segments. Raskin et al. (Raskin et al., 2008) add the body part histogram as an additional feature. Other authors use Visual Hull approaches (Laurentini, 1994) to work with voxel data. In that case, they can use three-dimensional flesh models, like ellipsoids (Mikic, 2003) or three-dimensional Gaussian mixtures (Caillette et al., 2005).

3 OUR APPROACH

3.1 Likelihood Evaluation

For the human body modelling we use an articulated model, which requires to be fleshed out in order to evaluate the likelihood of a given pose. In our approach we cannot rely on a 3D reconstruction that could be difficult to build and, indeed inaccurate. Therefore, a projection of the model onto the images is required. Our proposal is to avoid the computational cost of projecting the whole set of sampling points of a 3D flesh model by projecting a reduced set of points per body part. The flesh model will be a set of cylinders around all the skeleton segments except the head, which will be modelled by a sphere (see Fig.

3(a)). Therefore, our reduced set of projected points will be defined by the vertices of the trapezoidal section resulting from the intersection of a plane, approximately parallel to the image plane, with the cylindric shape modelling the limb (or spherical shape in the case of the head).

To define an intersecting plane for a given cylinder, we compute the vectors going from the camera center towards each one of the limit points of the limb. Then the cross product of these vectors with the one defined by the principal axis of the limb itself is computed to determine two normal vectors that lie on the intersecting plane and along which we will find the key points to project. The head template is handled with a similar procedure using as limb vector the one going from the base of the neck to the head center.

Regarding the image features, we propose modifications on a likelihood approximation like the one proposed in (Deutscher et al., 2000) while keeping common features that are easy to extract, like foreground silhouettes, edges and detected skin.

- We extract foreground silhouettes by means of a background learning technique based on Stauffer and Grimson's method (Stauffer and Grimson, 2000). A shadow removal algorithm (Xu et al., 2005), based on the color and brightness distortion, is used to enhance the segmentation.
- Edge detection is performed by means of the Canny edge detector (Canny, 1986). The result is dilated with a square 5x5 structuring element, and smoothed with a Gaussian mask. In order to avoid background spurious edges, we mask the edge detection provided by Canny's algorithm with a dilation of the foreground mask.
- A simple skin detection method based on evaluating the likelihood ratio between skin and non-skin hypothesis is performed. The likelihood functions are estimated by 8-bins color histograms of several skin and non-skin samples.

The final likelihood approximation will be a combination of several measures constructed with the aforementioned features.

N sampling points of the projected flesh model are matched with the extracted foreground. The weight is computed as follows:

$$\omega^{fl} = \frac{1}{N}\sum_{n=1}^{N}(1 - I_n^f) \tag{5}$$

Since pixel intensities in the foreground masks (I_t^f) have 0 or 1 as possible values, the weighting function is obtained by a normalized sum of the background pixels falling inside the projected flesh model. In the case of the head, we add skin detection information:

$$\omega^{fh} = \frac{1}{N}\sum_{n=1}^{N}(1 - I_n^f I_n^s) \tag{6}$$

Therefore, the final foreground weight ω^f is the averaged sum of all the limbs and head weights.

The proposed weighting function for edges is a sum of squared differences between the contour pixels and the edges of the flesh model aligned with the axis of the limb:

$$\omega^e = \frac{1}{N}\sum_{n=1}^{N}(1 - I_n^e)^2 \tag{7}$$

where N stands for the sampling points along the occluding edges of the projected flesh model.

3.1.1 Foreground Divergence Measure

The proposed foreground matching measure shows how well the model fits the observation, but does not evaluate how well the observations are being explained by the model. Suppose the likelihood $p(\mathbf{z}_t|\mathbf{x}_t)$ is available and that a given pose generates a pdf. A measure that can be used to assess the similarity of the likelihood and the generated pdf is the Kullback-Leibler divergence. At this point, it is important to remark that the KL divergence will provide different results depending on the factor order (except if both pdfs are identical). We can establish an analogy with our likelihood approximation. We are trying to determine the mutual information of the model and the observations. Therefore, we propose to include an additional divergence measure between the projection of the flesh model and the foreground masks to see how well a particle explains the observations.

$$\omega^d = \frac{1}{N_f}\sum_{n=1}^{N_f}(I_n^f(1 - B_n)) \tag{8}$$

This divergence basically consists in measuring the occupancy of the foreground silhouette (comprising N_f foreground pixels) by the B_n pixels of the projection of a given particle.

3.2 Feature-Based Annealing

The foreground matching measure produces a smooth and flat function (in almost every point) in which many different poses take considerable degrees of likelihood. However, foreground matching has the property of being discriminative with several wrong states. These properties can be observed in Fig. 1(a), where the weighting function is shown with actual data as a function of two angles. The foreground divergence measure is a smooth function that presents, in general, a broad global maximum (see Fig. 1(b)).

Edge matching is the most determinant measure in the sense that high values can only be reached when a particle is very close to the true pose. Nevertheless, spurious edges can also produce high values of the likelihood approximation (see Fig. 1(c)).

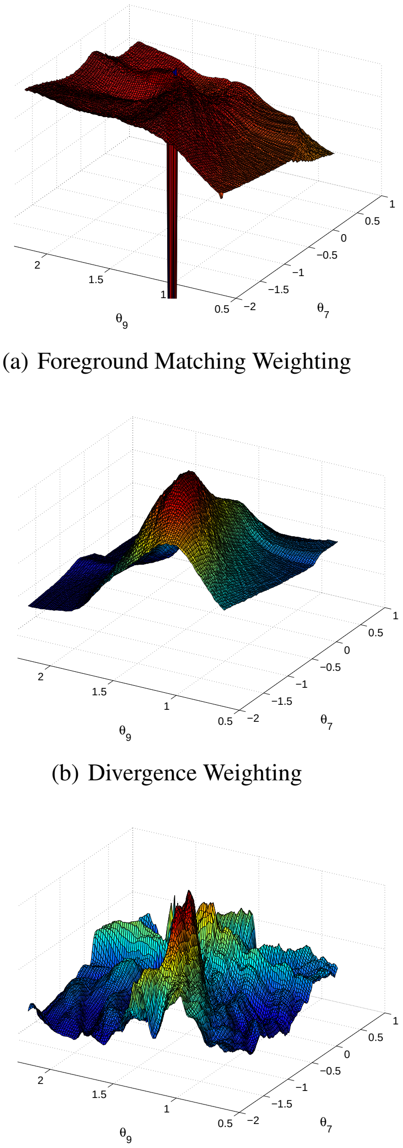

(a) Foreground Matching Weighting

(b) Divergence Weighting

(c) Edges Matching Weighting

Figure 1: Plots of the different feature weightings represented as functions of two angles of the left arm. The rest of parameters are set to values close to the true pose.

Since foreground measures produce very broad functions and edge matching tends to produce peaked functions, we can exploit annealing through the described attributes of the measures. We propose to use the annealing rate β not only as exponent of the likelihood approximation but also in the final average of all the measures derived from the image features:

$$\omega = exp\left(-\sum_{c=1}^{C}(\lambda_c^f(\frac{1}{\beta})\omega^f + \lambda_c^e(\beta)\omega^e + \lambda_c^d(\frac{1}{\beta})\omega^d)\right) \qquad (9)$$

where [illegible]he number of views and λ_c is a weighting coefficient depending on β (allowing to give more importance to foreground measures in the first layers and to edge measures in the last layers).

4 RESULTS AND DISCUSSION

4.1 Experimental Setup

We have tested our approach in an office desktop environment. During approximately two minutes, three subjects performed several common actions at a workplace (mouse dragging, writing, typing and picking objects). Hence, for our tests, we have focused on the upper body tracking.

Our setup was built under the premise of being portable, low cost and easy to configure. Two calibrated webcams, one frontal and one lateral, recording at 9.5 fps provided the frames onto which our body model has been projected (see Fig. 2). Both views are relatively close to the subject, thus the apparent size of some limbs in the image can change notably depending on their 3D position.

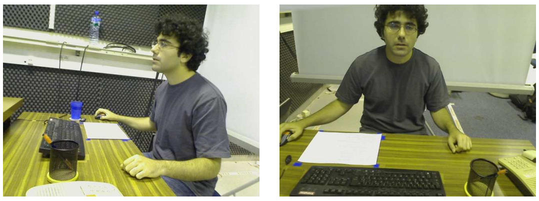

Figure 2: Available views for the experimental setup

4.2 Body Model

A simplistic articulated upper body model fulfills the requirements of the described scenario. This model is based on the kinematic chain framework (Bregler and Malik, 1998) and comprises a set of joints. In our case, this set of joints are the base of the neck,

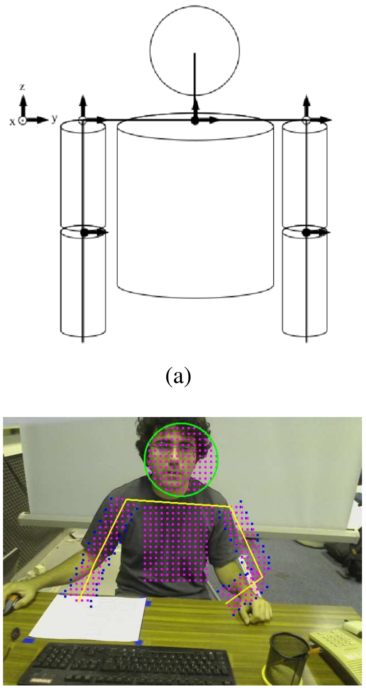

(a)

(b)

Figure 3: (a) Articulated upper body model and (b) its projection for a given particle

shoulders and elbows with a total of nine degrees of freedom. In order to set the model in a world position, a three-dimensional coordinate system built with the base of the neck as origin and a body orientation are defined. The world reference point for our model is set to be the base of the neck (see Fig. 3(a)). Therefore, the body model defines a thirteen-dimensional state vector:

$$\mathbf{x_t} = \{x_0, y_0, z_0, \theta_0, ..., \theta_9\} \tag{10}$$

Angle θ_0 is the orientation of the whole body model while all the other angles are designed following hard kinematic constraints.

4.3 Experimental Results

3D body part locations (head, shoulders, elbows and wrists) have been manually annotated in three sequences of three different subjects in order to test the tracker performance. The error is expressed as the mean distance between the annotated and the estimated joints.

Comparative results between the APF with the common likelihood approach (comprising edges and foreground matching) and our proposal are shown in Fig. 4. In both cases we used the body model and the projection procedure explained in section 3.1. Final mean error obtained by our approach for the three sequences was 104 mm, 74 mm below the common case for this difficult scenario. Common likelihood evaluation makes the tracker vulnerable to track loss, leading to higher mean error. On the other hand, the divergence measure and the feature-based annealing make the tracker more robust under these experimental conditions.

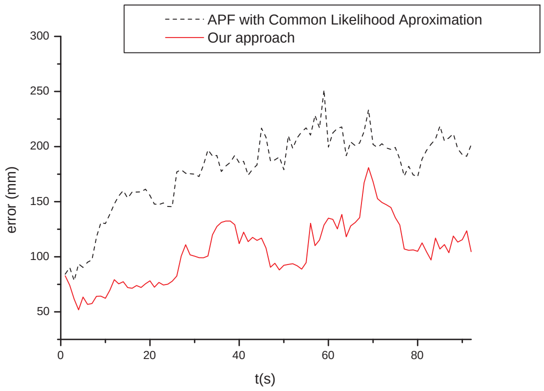

Figure 4: Comparative results using 3 layers and 200 particles per layer with the normal likelihood aproximation and our proposal.

We found out that some spurious edges due to clothing and objects caused our tracker to fail in its estimation. The apparent motion recorded in the images was very fast in some of the actions performed, causing blurs in the image and abrupt translation of body parts. Since the implemented annealing PF works with edges as the most determinant feature and has a simple propagation model, the algorithm was not able to track several of these fast motions. However, it was able to recover some poses after a tracking error.

5 CONCLUSIONS AND FUTURE WORK

We have presented an approach to exploit some common image features used in annealed particle filter techniques for human body tracking. We have introduced a foreground divergence measure that allows us to define a new procedure of annealing based on a decomposition of the likelihood approximation.

We have tested our proposal with a simple body configuration and a simplified projection method in a challenging scenario. A comparison between our proposal and existing methods has been presented. Some

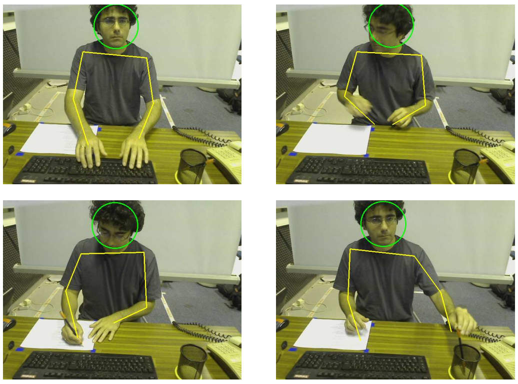

Figure 5: Tracking samples of a sequence where the subject types something in the keyboard, picks a pen, writes and leaves the pen again. The tracker is able to recover the pose after several errors due to fast apparent motion.

interesting results have been achieved in such conditions with a low number of particles and layers.

Like in the simple annealed particle filter we have tried to preserve the tracker generality by only adding hard kinematic constraints to our model. Consequently, our approach is not able to efficiently track fast apparent motions due to low frame rates. This could be attributed to a limitation of the state-space model and the common propagation model of the Sampling Importance Resampling framework from which annealing particle filter is derived.

Future research involves further validation of feature-based annealing with full body models and several recording conditions, and the extension of this study to other image features, including spatio-temporal features. The introduction of image features in the propagation scheme to avoid "blind" sampling with respect to the observations is another possible research line.

ACKNOWLEDGEMENTS

This work has been partially supported by the Spanish Ministerio de Educación y Ciencia, under project TEC2007-66858/TCM and by the European Commission under contract FP7-215372 ACTIBIO.

REFERENCES

Arulampalam, M., Maskell, S., Gordon, N., Clapp, T., Sci, D., Organ, T., and Adelaide, S. (2002). A tutorial on particle filters for online nonlinear/non-GaussianBayesian tracking. *Signal Processing, IEEE Transactions on*, 50(2):174–188.

Bregler, C. and Malik, J. (1998). Tracking People with Twists and Exponential Maps. *In Proc. CVPR (1998)*.

Caillette, F., Galata, A., and Howard, T. (2005). Real-Time 3-D Human Body Tracking using Variable Length Markov Models. *British Machine Vision Conference*, 1:469–478.

Canny, J. (1986). A computational approach to edge detection. *IEEE Transactions on Pattern Analysis and Machine Intelligence*, 8(6):679–698.

Canton-Ferrer, C., Casas, J., and Pardas, M. (2008). Exploiting Structural Hierarchy in Articulated Objects Towards Robust Motion Capture. *Lecture Notes in Computer Science*, pages 82–91.

Deutscher, J., Blake, A., and Reid, I. (2000). Articulated body motion capture by annealed particle filtering. *Computer Vision and Pattern Recognition, 2000. Proceedings. IEEE Conference on*, 2:126–133 vol.2.

Doucet, A., Godsill, S., and Andrieu, C. (2000). On sequential Monte Carlo sampling methods for Bayesian filtering. *Statistics and Computing*, 10(3):197–208.

Gordon, N., Salmond, D., and Smith, A. (1993). Novel approach to nonlinear/non-gaussian bayesian state estimation. *Radar and Signal Processing, IEE Proceedings F*, 140(2):107–113.

Isard, M. and Blake, A. (1998). CONDENSATION-Conditional density propagation for visual tracking. *Int. Journal of Computer Vision*, 29(1):5–28.

Laurentini, A. (1994). The visual hull concept for silhouette-based image understanding. *Pattern Analysis and Machine Intelligence, IEEE Transactions on*, 16(2):150–162.

Liu, J. and Chen, R. (1998). Sequential Monte Carlo methods for dynamical systems. *Journal of the American Statistical Association*, 93(5):1032–1044.

MacCormick, J. and Isard, M. (2000). Partitioned Sampling, Articulated Objects, and Interface-Quality Hand Tracking. *Lecture Notes in Computer Science*, pages 3–19.

Mikic, I. (2003). Human Body Model Acquisition and tracking using multi-camera voxel Data. *PhD. Thesis, University of California, San Diego*.

Mitchelson, J. and Hilton, A. (2003). Simultaneous pose estimation of multiple people using multiple-view cues with hierarchical sampling. *In Proc. of BMVC, September*.

Raskin, L., Rivlin, E., and Rudzsky, M. (2008). Using Gaussian Process Annealing Particle Filter for 3D Human Tracking-Volume 2008, Article ID 592081, 13 pages. *EURASIP Journal on Advances in Signal Processing*.

Stauffer, C. and Grimson, W. (2000). Learning Patterns of Activity Using Real-Time Tracking. *IEEE Transactions on Pattern Analysis and Machine Intelligence*, pages 747–757.

Xu, L., Landabaso, J., and Pardas, M. (2005). Shadow Removal with Blob-Based Morphological Reconstruction for Error Correction. *Acoustics, Speech, and Signal Processing, 2005. Proceedings.(ICASSP'05). IEEE International Conference on*, 2.